

---

# Investigating Source Conditions and Controlling Parameters of Explosive Eruptions: Some Experimental-Observational-Modelling Case Studies

---

Fabio Dioguardi, Tobias Dürig,  
Samantha L. Engwell, Magnus T. Gudmundsson and  
Susan C. Loughlin

Additional information is available at the end of the chapter

<http://dx.doi.org/10.5772/63422>

---

## Abstract

Explosive volcanic eruptions are complex systems that can generate a variety of hazardous phenomena, for example, the injection of volcanic ash into the atmosphere or the generation of pyroclastic density currents. Explosive eruptions occur when a turbulent multiphase mixture, initially predominantly composed of fragmented magma and gases, is injected from the volcanic vent into the atmosphere. For plume modelling purposes, a specific volcanic eruption scenario based on eruption type, style or magnitude is strictly linked to magmatic and vent conditions, despite the subsequent evolution of the plume being influenced by the interaction of the erupted material with the atmosphere. In this chapter, different methodologies for investigating eruptive source conditions and the subsequent evolution of the eruptive plumes are presented. The methodologies range from observational techniques to large-scale experiments and numerical models. Results confirm the relevance of measuring and observing source conditions, as such studies can improve predictions of the hazards of eruptive columns. The results also demonstrate the need for fundamental future research specifically tailored to answer some of the still open questions: the effect of unsteady flow conditions at the source on the eruptive column dynamics and the interaction between a convective plume and wind.

**Keywords:** explosive volcanic eruptions, convective plumes, eruption monitoring, large-scale experiments, numerical models

---

## 1. Introduction

The disruptive eruption of Eyjafjallajökull volcano in 2010 was a catalyst that has driven research agendas across disciplines from aeronautical engineering and satellite earth observation to social science and volcanology. In particular, there has been considerable focus on better observing and constraining the parameters of the 'volcanic source', which are used to initialise the flow field solution of most ash dispersal models used by Volcanic Ash Advisory Centres (e.g. [1, 2]). The volcanic source for ash dispersal models is generally a volcanic plume that is simulated with simplified models for obtaining plume properties (solid particles' mass/volumetric concentration, plume height and width, etc.). The plume evolution depends both on flow properties at the vent ('mass eruption rate' MER, which is the mass of ejected material per unit time and particles' properties like grain size distribution, density, shape and mass/volumetric concentration) and atmospheric conditions (e.g. wind and moisture vertical profile). Because of the considerable challenges inherent in measuring MER, it is usually indirectly inferred by applying empirical relationships or simplified models to measurements of plume height (e.g. [3, 4]). Such empirical models make a number of assumptions and are intended to simplify the system to support operational ash cloud forecasting. For example, for any given plume height, the mass eruption rate will vary depending on eruption type and meteorology [5, 6] giving rise to errors of up to a factor of 4 [3]). In some meteorological circumstances errors may be even larger if, for example, deep moist convection resulting in much larger plume heights than expected (e.g. [6–8]). In addition, there is an urgent need to better understand the controls on eruption column collapse that can generate pyroclastic density currents.

Developments in modern technology allow both qualitative and quantitative time-series observation of volcanic plumes (e.g. plume height, temperature, etc.), enabling variation with time to be observed in detail (e.g. [9–12]). Due to the non-steady nature of the process, monitoring dynamic source conditions (e.g. MER) at vent remains a difficult task. Here we use the recent innovations of Dürig et al. [13, 14] to highlight ways in which emerging techniques can be used to better understand source processes. Dürig et al. [13, 14] established a means of quantifying the mass eruption rate of individual explosive pulses at the vent based on high-resolution imagery (optical and thermal) of the Eyjafjallajökull eruption. Their technique can be applied in near real-time to monitor the changing mass eruption rate. They embraced the complexity of the eruption by studying the pulsatory explosive source in detail. Interestingly, they found that simple 1D models predict similar plume heights, even for a pulsatory eruption.

Experimental studies are a means of controlling conditions to isolate and investigate particular parameters and/or processes. We summarise a series of large-scale experiments of explosive eruptions, which have enabled identification of new parameters and have quantified controlling factors in changing regimes between eruption types (e.g. collapsing columns and convective plume). We propose the next steps in experimental volcanology including the representation of a pulsatory source and interaction with wind.

Finally, we summarise recent advances in plume rise modelling, in particular the recent model intercomparison study. These studies show that a key weakness in modelling volcanic plumes, is the treatment of the effects of the wind on the rising plume. Finally, we highlight how such

weaknesses may be addressed using a combination of numerical modelling and experimental studies.

Better understanding of the source conditions and how these affect the development and evolution of eruptive plumes is essential to reduce uncertainties in ash dispersion modelling and facilitates forecasting of ash fall and pyroclastic density current hazards. In this chapter, we propose that a combination of improved observations, experiments and modelling will initiate a step change in the way scientists can contribute to risk reduction in near real-time. We present three case studies and their results to demonstrate both the outstanding issues and potential solutions.

## **2. Insights from observations: case study 1—determination of the mass eruption rate of a pulsating eruption (Eyjafjallajökull 2010)**

In May 2010, Martin Rietze, a bold German photographer climbed to the top of the Icelandic volcano Eyjafjallajökull on three subsequent days and managed to mount his camera a mere 850 m from the vent, before taking cover behind a large rock, which Icelanders call “Goðasteinn” (God’s rock). Fortunately, he and his camera survived these risky missions, providing the volcanological community with close-up footage of explosive activity at the vent. The Eyjafjallajökull eruption 2010, which received broad international attention because of the disruptive consequences on aviation in large parts of Europe, initiated with “wet” phreatomagmatic explosive activity from 14th to 18th April [15]. After a short period of significantly decreased discharge rate and mixed effusive-explosive activity, on 5th May the eruption entered a second explosive stage, which was “dry” and purely magmatic [15, 16]. This stage was characterised by repetitive closely timed explosions, each resulting in the release of discrete ash pulses [10, 17]. The repetitive explosions continued for over 2 weeks with a decline in eruptive activity between 17 and 21 May and the end of continuous eruptive activity recorded on 22nd May [15]. From a distance, and particularly downwind, the rising plume appeared quasi-steady and sustained throughout this stage of the eruption. Measurements made by a thermal camera mounted at a distance of 8.3 km from the vent on 4th May revealed average initial pulse velocities of  $45 \text{ m s}^{-1}$  and average pulsation intervals  $t_{\text{pulse}}$  of  $\sim 20 \text{ s}$  (see **Table 1** for Notation), meaning that on average three pulses occurred every minute [17]. However, the ash pulses within the footage taken 4, 5 and 6 days later showed an increase in the average initial vertical velocities to  $65 \text{ m s}^{-1}$  and—even more prominent—a significant drop of the average pulsation interval  $t_{\text{pulse}}$  to 4.2 s, coinciding with the significantly increased overall mass flux [13]. Furthermore, these video analyses revealed that two types of explosive pulses could be discriminated by their observed diameter at the vent exit: ‘strong’ pulses, featuring diameter at a vent of greater than 50 m and ‘weaker’ pulses, characterised by a diameter at the vent exit of less than 50 m [13]. The two types also significantly differed in their rate of occurrence: the time between weaker pulses ( $t_{\text{pulse}}$ ) was on average 4.7 s and between strong pulses on average of 37.5 s [13]. Studies of ejecta trajectories enabled characterization of the vent as a funnel with a depth of  $51 \pm 7 \text{ m}$ , an inner diameter of 8–15 m and an outer diameter (8–10 May) of  $65 \pm 2 \text{ m}$  [14]. The inner vent is the surface from which the column starts to expand

(intersection point of ballistic profiles) but is not the same as the site of magma fragmentation, which is probably deeper. These studies indicated that the “weaker” pulses can be seen as punctuating jets that are sourced from areas of only  $\sim 8$  m diameter in the ‘inner vent’, whereas the ‘stronger’ pulses occupy a greater area of the inner vent [14].

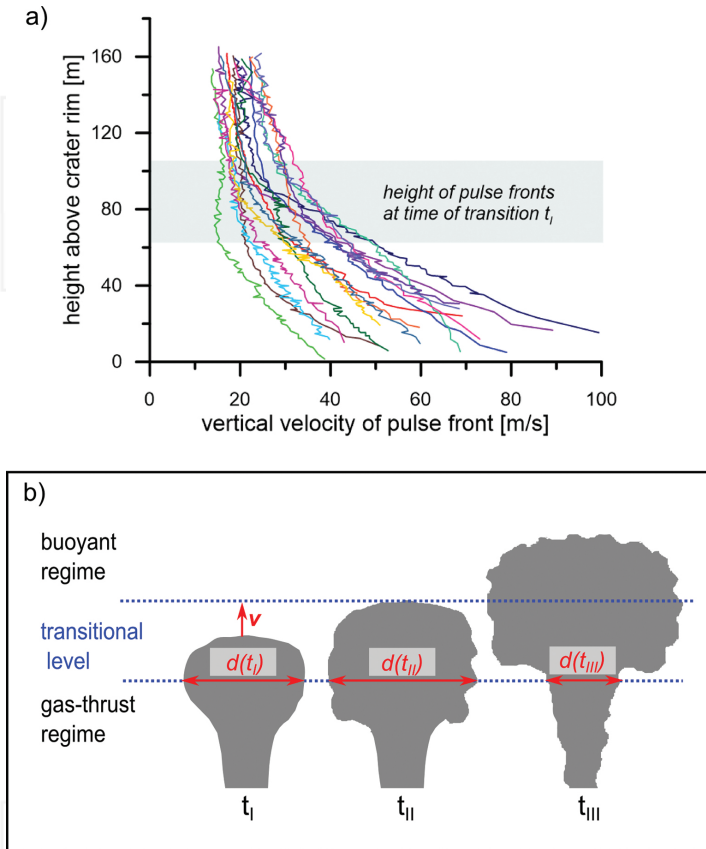


**Figure 1.** Temporal evolution of an ash pulse. (a) Vertical velocities of 16 pulses of the Eyjafjallajökull 2010 eruption. When entering the transitional level between gas-thrust and buoyant regime, many velocity curves show a clear “kink,” a phenomenon that has previously been reported for other eruptions, e.g. Patrick et al. [19] and Marchetti et al. [20]. The moment of change in dynamic behaviour is defined as  $t_i$ . (b) The elevation of the maximum pulse width  $d(t_i)$  determines the position of the lower boundary of the transitional level, which is used as a reference plane for estimating the mass flux by the pulse velocity-derived model (PVDM). The upper boundary is defined by the elevation of the pulse front at the moment  $t_{iII}$ , when the pulse width  $d(t)$  shows its maximum extension. After that, moment  $d(t)$  decreases. As a cut-off criterion, the end of the ash transport through the reference plane is defined by the moment  $t_{iIII}$ , when the width has dropped to  $d(t_{iIII}) = d(t_i)e^{0.5}$ . Copyright Dürig et al. [13], published by SpringerOpen.

Based on these findings, a pulse velocity-derived model (PVDM) was developed [13]. This model determines the mass flux contribution of individual ash pulses analysed in the videos in order to estimate the overall MER. The starting point of the PVDM is the temporal evolution

of individual ash bursts, which can be summarised as follows: a pulse exits the vent as a momentum-driven negatively buoyant jet, which expands during its rise due to entrainment of ambient air, before finally reaching a transitional level. At this level, buoyancy takes over as the dominant uplift mechanism, generating a convecting plume as the bulk density of the gas-particle mixture making up the pulse approximates the density of ambient air (e.g. Sparks [18]). As reported for other eruptions [19, 20], the videos of the Eyjafjallajökull eruption showed that the vertical velocities of the pulse fronts dropped with height until entering the level of transition. At this point, the vertical velocity curves are characterised by a distinct kink (see **Figure 1a**), showing a constant uplift velocity within the subsequent buoyancy-driven stage.

Change in the vertical velocity profile can be used to identify the moment of transition into the buoyant stage,  $t_I$ . The maximum pulse width  $d(t_I)$  defines the lower boundary of the transitional level (see **Figure 1b**). With ongoing pulse evolution,  $d(t)$  increases until it reaches a maximum  $d(t_{II})$ . The upper boundary of the transitional level is defined by the elevation of the pulse tip at  $t_{II}$ . Following this key assumption, the density of the gas-solid mixture  $\rho$  in the zone of transition can be approximated to be equal to that of the surrounding air. With this parameter known, the volume fraction  $C$  of solids within a pulse made of a mixture of gas (density  $\rho_g$ ) and tephra (density  $\rho_t$ ) can be computed by:

$$C = \frac{\rho - \rho_g}{\rho_t - \rho_g} \quad (1)$$

The mass flux  $Q(t_I)$  of a pulse can be approximated as that of a homogenous gas-particle mixture with a velocity  $v$  through a cylindrical cross-section of the diameter  $d(t_I)$ .

$$Q(t_I) = \rho_t \cdot C \cdot \left( \frac{d(t_I)}{2} \right)^2 \cdot \pi \cdot v \quad (2)$$

while the vertical velocity  $v$  can be estimated by tracking the pulse tip between  $t_I$  and  $t_{II}$ , the temporal change in diameter  $d(t)$  complicates the calculation of the time-dependent mass flux  $Q(t)$ . Dürig et al. [13] suggested bracketing the mass flux by calculating two end-members, representing the range of possible values. Therefore, they specified the duration  $\tau$  for which the mass flux has decreased by a factor of  $1/e$ , with  $\tau = t_I - t_{III}$ , where  $t_{III}$  is the moment when the pulse diameter at the lower transitional boundary has decreased to  $d(t_I)/e^{0.5}$  (see **Figure 1b**). The lower and the upper limit of the mass flux of tephra,  $Q_{min}$  and  $Q_{max}$  can then be estimated by:

$$Q_{min} = \frac{\tau}{t_{pulse}} \cdot Q(t_I) \cdot (1 - 1/e) \quad (3)$$

$$Q_{max} = \frac{\tau}{t_{pulse}} \cdot Q(t_I) \quad (4)$$

The PVDM provided MER estimates of  $2.2\text{--}3.5 \cdot 10^4 \text{ kg s}^{-1}$  for the period studied [13]. These values have been shown to be in good agreement to those resulting from simple 1D plume models and empirical relationships fed by plume height data observed for 8–10 May (2.9–3.3 km above vent). For example, the model of Wilson and Walker [21] suggests  $2.3\text{--}3.8 \cdot 10^4 \text{ kg s}^{-1}$ , Sparks et al. [5] estimates  $2.2\text{--}3.5 \cdot 10^4 \text{ kg s}^{-1}$  and Mastin et al. [3] predicts  $1.2\text{--}2.1 \cdot 10^4 \text{ kg s}^{-1}$ . Gudmundsson et al. [15], who calibrated the Mastin model for Eyjafjallajökull 2010 using a scaling factor adjusted to mapped fallout, suggest MER values of  $1.9\text{--}3.3 \cdot 10^4 \text{ kg s}^{-1}$  for 8–10 May.

Interestingly, according to the results of the PVDM, the greater part (78%) of the total mass flux on 8–10 May was provided by the frequent pulses of the “weaker” type, despite the fact that the less frequent “strong” pulses each transported, on average, 2.3 times more mass of tephra than a ‘weak’ pulse. These findings underline the need to consider the whole spectrum of explosive pulses when applying the PVDM. The good agreement between the models can be seen as an indication that the “simple” 1D models and empirical relations work also for pulsating eruptions—and that near-field observation based models, such as the PVDM, provide a possibility to quickly estimate the overall mass flux in near real-time.

The application of this new observational technique helped researchers to better constrain source conditions, in particular to better estimate the mass of ejected particles and MER even in unsteady conditions. The next challenge is to apply this method in near-real-time.

Due to the innate complexity of the phenomena taking place during explosive eruptions, it is hard both to monitor all the aspects of the multiphase flow at the source (e.g. particle concentration) and to relate these flow field variables to the observable dynamics. For this reason, large-scale experiments aimed at reproducing constrained eruptive regimes and defining scaling laws between source conditions and the erupted plume represent a powerful tool towards a better and more comprehensive understanding of explosive eruptions.

### 3. Insights from large-scale experiments on eruptive columns: case study 2 — source conditions (single pulse of variable duration) and eruptive regime

#### 3.1. Overview of experimental apparatus and runs

The highly complex nature of the phenomena that occur during explosive eruptions means that prior to early 2000 experimental research in volcanology was limited to small laboratory scale experiments that did not reach a scale comparable to natural phenomena [22]. In this section, the results of the first large-scale experiments carried out between 2005 and 2009 by researchers from the University of Bari (Italy) and the University of Würzburg (Germany) are summarized [23–26]. In particular, relationships between eruptive regimes and source

conditions obtained by experiments and their application to hypothetical natural-scale eruptions are presented. In the following years, the importance of achieving large-scale conditions when reproducing the processes that take place during explosive has been realised. Following the pioneering results described here, new large-scale experimental facilities were developed [27, 28]. One of the reasons for this large scale is that, as gas-particle coupling is influenced by the shape and size of volcanic particles [23], the dimension of the experimental facility needs to be sufficiently large to allow the use of real volcanic particles sampled from tephra deposits. The other reason is that, in order for the reproduced volcanic flows (conduit, eruptive column, pyroclastic flow) to be comparable to natural phenomena from a fluid dynamic point of view, their Reynolds number ( $Re$ ) needs to be of a similar order of magnitude or at least scalable. In turn,  $Re$  depends directly on a characteristic dimension and velocity of the flow, thus the larger the setup and the faster the generated flow, the closer  $Re$  is to that of natural flows.

The experimental apparatus used in the modelling is fully described in recent papers [23–26] and schematized in **Figure 2**.

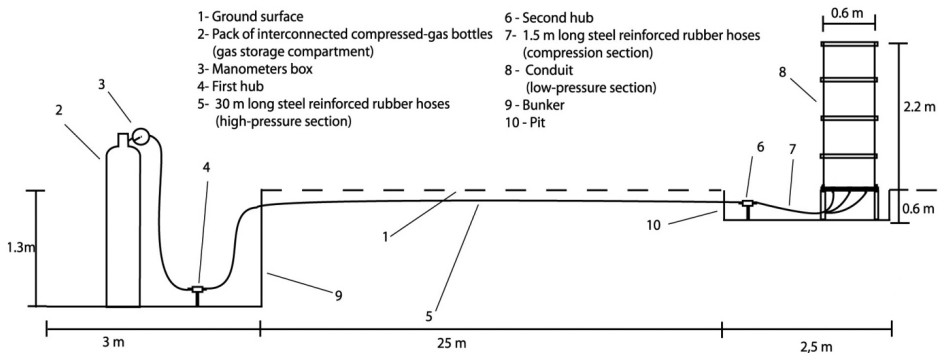


**Figure 2.** Schematic representation of the experimental apparatus. Copyright 2007 by the American Geophysical Union. Reprinted by permission of John Wiley & Sons, Inc.

Briefly, the model setup was designed to achieve coupling between an applied mechanical energy and ash and lapilli particles in a vertical conduit. Both cold and hot (up to 300 °C) ash and lapilli were used to investigate the role of temperature in plume dynamics. Mechanical energy was provided by expanding overpressured gases in rubber tubes connected to the conduit; when expanding, the gas coupled with the particles in the conduit, generating a multiphase flow. The time scale of mechanical energy release was forced to be similar to that of the mechanical energy release during magma fragmentation experiments [29, 30]. Accounting for the link between gas and particle acceleration with magma fragmentation in the conduit in real eruptions [24]. Depending on experimental conditions, this multiphase flow produced different eruptive regimes: collapsing columns (generating pyroclastic density currents), convective plumes, radially expanding jets and transitional regimes between these extremes

(**Figure 3**). The experimental facility allowed complete control of eruptive regime. Specifically, the ratio between the total expansion energy  $E_{tot}$  (given by the product of the driving pressure  $\Delta P$  and the gas volume  $W$ ) and the particle mass load  $m$ , known as specific mechanical energy (SME) [23], was crucial in determining eruptive regime. After the first experimental runs, threshold values for this parameter were obtained: when  $SME > 2.6 \text{ kJ kg}^{-1}$  a dilute column evolving as a convective plume was generated (**Figure 3a**); in comparison, when  $SME < 1.5 \text{ kJ kg}^{-1}$  a dense column was reproduced which, depending on conduit exit overpressure, could evolve either as a collapsing column or an overpressured radially expanding jet (**Figure 3b and c**). Transitional behaviours were reproduced for intermediate values of SME (**Figure 3d**).



**Figure 3.** The four different eruptive styles reproduced in the experiments. (a) Convective plume. (b) Collapsing fountain generating a pyroclastic density current. (c) Overpressured radially expanding jet. (d) Transitional style between convective plume and collapsing column.

### 3.2. Source conditions controlling the evolution of eruptive columns

While SME is a fundamental parameter controlling the eruptive regime of the experiments, due to its functional form it does not have a practical use for forecasting or even describing real eruptive regimes. For this purpose, parameters strictly linked to source conditions at vent (conduit exit) that can be reasonably hypothesised for future eruptions and/or measured during ongoing eruptions (e.g. exit velocity) are of fundamental importance.

Discriminating between different eruptive regimes is not merely a scientific exercise but has important implications in hazard assessment of explosive eruptions, as each style is responsible for particular hazards (e.g. the injection of fine ash into the atmosphere by plumes or the formation of pyroclastic density currents from collapsing columns). Thus, source parameters have been investigated using measured experimental data.

From data recorded during the experiments, both new parameters and those that are already used in fluid dynamics and volcanological literature have been measured. In particular, three parameters were identified as being crucial for describing the activity observed during an eruption. The first parameter was newly defined for discriminating between dilute (**Figure 3a**) and dense collapsing columns (**Figure 3b–d**). It is well established that the formation of convective plumes is favoured by high exit velocities  $U_0$ , low particle concentration  $C_0$  and small vent radius  $r_0$  and vice versa for collapsing columns [24, 31]. These variables have been combined to obtain the following parameter:

$$\Omega = \frac{2U_0}{r_0 C_0} \quad (5)$$

Where 2 derives from the ratio between column surface area and volume, which is  $2/r_0$  for a cylinder. This ratio is fundamental for the entrainment of external air into the column. In the experiments,  $U_0$  was measured by video analysis, whereas  $C_0$  was inferred assuming a complete dilution of the volume of ash in the conduit.  $\Omega$  is dimensionally analogous to vorticity ( $s^{-1}$ ), thus it can be seen as a measure of turbulence intensity in the column. In its functional form, the higher  $\Omega$  (the more intense the turbulence), the more likely a convective plume will be generated. This is not surprising, as turbulence enhances air entrainment into the column, the main process leading to the formation of a convective plume [32].

The second parameter was defined for discriminating between vertically evolving columns (both plumes and collapsing columns) and radially expanding jets. Radially expanding jets are typical of phreatomagmatic eruptions, where magma fragmentation occurs on interaction with groundwater at shallow levels in the crust [33]. The short distance between the location at which wet fragmentation typically occurs and conduit exit causes the eruptive mixture to exit from the vent with a static overpressure in respect to atmosphere [34, 35]. Thus, the eruptive mixture expands in all directions as it equilibrates to atmospheric pressure and dilutes pyroclastic density currents form. This process has been reproduced in experiments by shortening the conduit. From these considerations, a regime parameter  $\Gamma$  designed for discriminating between over-pressured and pressure-balanced eruptive columns should combine static exit overpressure  $P_{over,0}$  and dynamic pressure  $P_{dyn,0}$  (which favours vertical columns) at the source:

$$\Gamma = \frac{P_{0}}{P_{dyn,0}} = \frac{P_{st,0} - P_{atm}}{P_{dyn,0}} \quad (6)$$

where  $P_{st,0}$  is the static pressure at conduit exit, which is extrapolated from the static pressure measured by the pressure sensor positioned close to the experimental conduit exit;  $P_{dyn,0}$  is half of the product between mixture density (a function of  $C_0$ ) and the squared exit velocity. By its definition, the higher  $\Gamma$ , the more likely a radially expanding jet is generated.

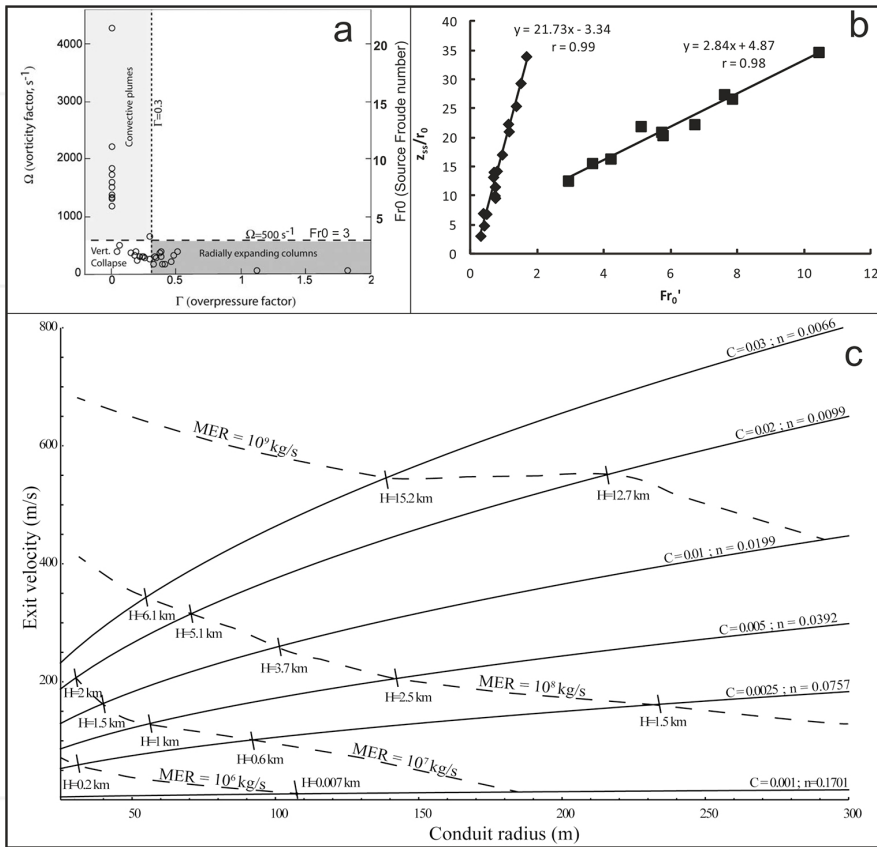


**Figure 4.** (a) Regime stability field of experiments as a function of  $Fr'_0$ ,  $\Gamma$  and  $\Omega$ . Small white area corresponds to the field of vertical collapse; light grey area is the convective plume stability field, whereas dark grey area corresponds to radial expanding columns (b)  $z_{ss}$  vs.  $Fr'_0$  diagram; diamonds and square represent dense-collapsing columns and dilute convective plumes, respectively. Fitting lines are also traced. Note that data points here are less numerous than in Figure 4a, as it was not possible to measure  $z_{ss}$  for all the experiments. (c) Regime diagram showing exit velocity ( $U_0$ ) vs. conduit radius ( $r_0$ ) for real-scale eruptions. Solid lines represent different values of particle volumetric concentration  $C_0$  (or the corresponding mass fraction  $n$ ) at source; dashed lines represent different values of mass eruption rate (MER). “Bulletin of Volcanology, Volcanic jets, plumes, and collapsing fountains: evidence from large-scale experiments, with particular emphasis on the entrainment rate, 76, 2014, 834, Dellino P., et al., © Springer-Verlag Berlin Heidelberg 2014. With permission of Springer”

The third parameter, the densimetric Froude number  $Fr'_0$ , originates from published literature on the fluid dynamics of jets and fountains:

$$Fr_0' = \frac{U_0}{\sqrt{g_0' r_0}} = \frac{1}{\sqrt{Ri}} \quad (7)$$

Where  $g_0'$  is the reduced gravity, a function of gravitational acceleration and density contrast between the flow and air at the source;  $Ri$  is the Richardson number.  $Fr_0'$  has been used in fluid dynamic literature as the parameter controlling the regime of flows issuing from circular nozzles [36, 37] and, later, in volcanology for similar purposes [38, 39].  $Fr_0'$  was also found to influence the entrainment rate in the jet [40].

$\Omega$ ,  $\Gamma$  and  $Fr_0'$  have been evaluated from data recorded during the experimental runs and their threshold values discriminating different eruptive regimes were inferred by plotting their values on charts. In **Figure 4a**, an experimental regime diagram is displayed: the two y-axes represent  $\Omega$  and  $Fr_0'$ , whereas  $\Gamma$  is on the x-axis. Lines representing the threshold values are also traced. In particular, the experiments showed that when  $\Omega > 500 \text{ s}^{-1}$  a convective plume forms, otherwise a collapsing column or radially expanding jets develops. The stability fields of these last two eruptive regimes are divided by the line  $\Gamma = 0.3$ , with radially expanding jets lying in the area  $\Gamma > 0.3$ . Finally, the threshold value for  $Fr_0'$  is also reported (3), which acts similarly to  $\Omega = 500 \text{ s}^{-1}$ , with convective plumes forming when  $Fr_0' > 3$ . This last threshold value has been obtained in a slightly different way. In **Figure 4b**, experimental results are plotted in a diagram  $z_{ss}/r_0$  vs.  $Fr_0'$ , where  $z_{ss}$  is the steady state height of the column [26, 41]; squares and diamonds represent convective plumes and collapsing columns, respectively. In agreement with the fluid dynamics literature of jets [37, 42], the two types of experiments follow very different linear trends, and a threshold value of  $Fr_0' = 3$  can be identified.

These findings allowed the production of regime diagrams for hypothetical real eruptions [26]. One example is shown in **Figure 4c**, in which solid lines represent different values of particle volumetric concentration  $C_0$  (or the equivalent solids' mass fractions  $n$ ) at the threshold condition  $Fr_0' = 3$ . For each line, the area above it is the plume stability field, while the area below it represents the collapsing column stability field. The dashed lines represent different values of source mass eruption rate (MER).

The regime diagram agrees well with volcanological theory and observations. Given a conduit radius and fixed a source particle volume fraction, the higher the exit velocity, the more likely the formation of a convective plume [43]. The collapsing column stability field expands as source particle volumetric concentration and conduit radius increase. Furthermore, this regime diagram is in very good agreement with other diagrams obtained from numerical simulations [26, 38–40], proving that both experiments and models are valuable tools for gaining insights into the dynamics of these complex phenomena.

Results show how eruptive regimes are strongly controlled by source conditions. This is not surprising: in particular, the influence of the source Froude number on eruptive column conditions agrees very well with classical fluid dynamic theory of jet and plumes issuing from circular nozzles. Large-scale experiments confirm that applying such concepts to eruptive columns (for example, for computing the trajectory of a convective plume) is a good approximation and that experiments scale well with real eruptions.

### 3.3. The role of air entrainment in eruptive dynamics

The generation, regime and evolution of an eruptive column are not only controlled by source conditions but also by other fundamental processes (gas condensation, entrainment, particle segregation, etc.). Among these, entrainment of external air into the eruptive column by the action of turbulent eddies plays a crucial role [32, 44]. Once entrained air is in contact with hot gases and volcanic particles in the eruptive mixture, it heats and expands, reducing the column's bulk density and contributing to its radial expansion and ascent. This process is particularly important in the dynamics of convective plumes. The concept of entrainment was formalised by Morton et al. [32], who introduced entrainment velocity in their simplified steady 1D model of buoyant plumes. Entrainment is a process linked to turbulence and is thus inherently three-dimensional (3D) and unsteady. For this reason, entrainment has to be parametrized in order for it to be taken into account in simplified steady 1D models. Entrainment velocity is defined as the volume flow rate per unit area of external air entering into the plume and is directly proportional to plume vertical velocity. The constant of proportionality is the so-called entrainment coefficient  $\alpha$ .

The entrainment coefficient appears explicitly in the mass and energy conservation equations of 1D plume models. These models are widely employed in volcanology, in particular for initializing ash dispersal simulations [2, 45] or, by inversion, for estimating source conditions from observations (e.g. [4]). The importance of an accurate estimate of  $\alpha$  is therefore evident. Fortunately, there is substantial agreement on the value of  $\alpha$ , with values of about 0.09–0.1 usually considered to be reliable [37, 40, 44]. Recently, some authors introduced variable entrainment coefficient laws, with entrainment being a function of Froude number (thus of density contrast between plume and atmosphere) and complex height-dependent coefficients [39, 40]. The dependency of  $\alpha$  on density contrast is not surprising: it is well established that the higher the density contrast, the lower the entrainment [46]. Thus, the use of variable entrainment coefficients allows more realistic simulations of convective plumes.

This is confirmed by large-scale experiments. A method has been devised that, from analysis of the spreading rate of experimental eruptive columns, allows the quantification of entrainment velocity [26] and, from measurements of plume vertical velocity,  $\alpha$ . For hot dilute convective plumes (**Figure 3a**), an average value of 0.11 was determined, in agreement with values reported in the volcanological literature. Interestingly,  $\alpha$  has been found to vary with experimental eruptive regime: average values of 0.06 for cold plumes and transitional columns (**Figure 3d**) were calculated (which agree with the values of pure jets in fluid dynamics [36, 37, 40]), whereas for collapsing columns (**Figure 3b**)  $\alpha$  was always negligible. A collapsing column can thus be considered as an incompressible fluid, whose trajectory is completely described by the Bernoulli equation. This approximation enables the maximum height reached by a collapsing column to be obtained from source conditions (bulk density and velocity) and is a measure of potential energy that is converted to kinetic energy at collapse. From these considerations, it is possible to infer initial and boundary conditions of pyroclastic flows, starting from source conditions of collapsing columns.

Large-scale experiments confirmed the importance of entrainment coefficient not only in the dynamics of convective plumes but also in the generation of a specific type of explosive

eruption. As aforementioned, a number of other parameters play a role, especially in convective plume dynamics. The relative importance of different parameters, particularly when applying 1D numerical model to simulate volcanic plumes, is further discussed in Section 4.

### 3.4. Future perspectives

While these experiments provided key insights into important parameters controlling the eruptive regime, their design did not allow to investigate other fundamental processes controlling the evolution of eruptive columns. In particular, the experiments were characterised by a single pulse, although of variable duration, of ejected eruptive mixture. Section 2 has stressed the importance of taking into account other possible flow patterns at the source, like pulsating mass flux, and a new method for quantifying the mass eruption rates of eruptions characterised by a pulsating source has been presented. A verification of this model using large-scale experiments would represent a further necessary step, also in the view of finding empirical relationships between eruptive column characteristics (e.g. height) and pulsating source properties.

Furthermore, these experiments were not designed for studying the interaction between convective plumes and wind. Wind plays a major role in controlling the convective plume trajectory [4, 39, 47–51] for two reasons: (1) it enhances air entrainment, by the addition of a wind-induced tangential component to the already mentioned radial one and (2) it bends the plume trajectory (hence affecting plume height), especially of weak plumes. As plume height is influenced by the presence of wind and is used for inferring the source MER, it is evident how wind effects should not be neglected, in particular for weak plumes. New experiments specifically designed for investigating plume-wind interactions would be of fundamental importance, especially for assessing the wind entrainment rate, which is currently the most uncertain parameter in simplified models of bent-over plumes.

## 4. Insights from modelling: case study 3—results from sensitivity analyses of numerical plume models

As with many other physical phenomena, numerical models have been employed to understand the processes that occur during explosive volcanic eruptions (a range of models can be found on the open access platform VHuB [52]). Specifically, a number of models have been developed to simulate plume rise into the atmosphere, with such models commonly used to determine appropriate input parameters for ash dispersion models. Two types of model exist, one-dimensional integral models, which evaluate plume rise along a centre line, solving equations for conservation of mass, momentum and thermal energy along that line (e.g. Plumeria: Mastin [6]; PlumeRise: Woodhouse et al. [49]; PlumeMom: de' Michieli Vitturi [53]), and 3D models, which account for more complex interactions between the rising plume and the atmosphere (e.g. ATHAM: Herzog et al. [54]; ASHEE: Cerminara et al. [55]). One-dimensional models are often used in an operational sense in the event of an eruption because they are quick to employ and, due to the simplicity of the models they require less detailed

knowledge of, for example, atmospheric conditions. However, the simplicity of these models means that establishing important plume dynamics, and characteristics, for example the neutral buoyancy height, and the behaviour of the plume above the height of neutral buoyancy is not possible.

As mentioned above, one-dimensional numerical models are commonly used to estimate the maximum plume height and the mass flux at this height. Inputs for these models include atmospheric conditions (temperature, density and pressure with height), initial vent radius, eruption velocity and temperature (which together describe eruption mass flux), and particle characteristics (grain size, particle density and drag coefficient and the settling law to be employed). Further key parameters are those that describe entrainment of ambient air into the plume, both by simple turbulent entrainment and by interaction with wind as mentioned above in Section 3.3.

Following the ash dispersion model intercomparison study [2], Costa et al. [45] led a plume model intercomparison study to identify key differences between plume models. The intercomparison study involved 13 models: 9 one-dimensional and 4 three-dimensional models. Each model was applied to a bent-over plume (based on the Shinmoedake eruption of 2011) and a vertical plume (based on the climatic eruption of Pinatubo 1991) example. The aim of the exercise was to determine the cases in which the different models perform best and to highlight areas for future research. Results from the one-dimensional models were consistent, unsurprising given that all of the models are based on the mathematical description of turbulent buoyant plumes by Morton et al. [32], and were also largely consistent with results from three-dimensional models. While there are discrepancies on a local scale between 1D and 3D models for the vertical plume example, predicted plume heights are similar, highlighting the utility of 1D models for operational means [45]. The greatest discrepancy in results occurred when weak plumes erupting into a crosswind were modelled, with a 20% difference in modelled plume height results.

A key result from the exercise concerned the treatment of entrainment by the models. As described above, interaction between a volcanic plume and ambient wind leads to enhanced entrainment of air, and horizontal momentum, plume bending and a decrease in the maximum plume height for a given mass eruption rate [47]. Within the models, the effect of wind on entrainment is described by:

$$U_e = \alpha |U - V \cos \vartheta| + \beta |V \sin \vartheta| \quad (8)$$

Where  $\vartheta$  is the angle between plume centreline and the horizon,  $\alpha |U - V \cos \vartheta|$  describes the radial entrainment minus the amount swept tangentially along the plume margins,  $\beta |V \sin \vartheta|$ ; describes the entrainment due to wind,  $\alpha$  describes the radial entrainment coefficient and  $\beta$  is the wind entrainment coefficient [47, 56]. There is substantial agreement among the different bent-over plume models on combining radial and tangential entrainment components in this linear way, but other nonlinear combination have also been proposed [57]. As mentioned above, the radial entrainment coefficient is well defined in the literature. Laboratory experi-

ments [56] have shown the wind entrainment coefficient to be near unity, but this value is much less well constrained than for radial entrainment; in fact, its value varies from about 0.5 to 1 in the literature [4, 39, 47–51]. Results from the intercomparison exercise indicate that 1D models fail to reproduce entrainment for large plumes, despite providing reasonable estimates of column height. Results from a number of recent studies highlight the importance of entrainment, and particularly that associated with wind, in controlling behaviour of volcanic plumes, for example whether plume collapse occurs or not [26, 39, 48, 49, 51, 57]. Modelling studies have also shown that in some cases, increase in entrainment associated with eruption into wind leads to a plume that would otherwise collapse to become buoyant.

A number of the studies that contributed to the intercomparison exercise used formal sensitivity techniques to evaluate the performance of the models, and specifically the manner by which uncertainties in input parameters affect model output uncertainties. Sensitivity analysis is used to show how variation in model output can be attributed to different sources of uncertainty in model inputs. Such analysis enables key model parameters to be identified, such that they can be studied with greater depth than those parameters that have little influence on model results. Application of this technique requires identification of an appropriate probability density distribution for each input parameter. The model is run a number of times, with each simulation sampling the input distributions such that the entire parameter space is sampled, and model response to varying input parameters can be statistically evaluated. Application of sensitivity analysis by de' Michieli Vitturi et al. [58] and Woodhouse et al. [50] to one-dimensional plume models highlight the dependence of model results not only on source mass flow rate (described by exit velocity, temperature and water fraction), but also the input entrainment assumptions, and in particular the entrainment associated with wind.

## 5. Conclusive remarks

Results from experiments, observations and models highlight the fundamental role played by source conditions at the vent in the dynamics of explosive eruptions and dispersion of ash clouds. Large-scale experiment results demonstrate a quantitative link between eruptive characteristics and source conditions, by means of new (e.g. vorticity and overpressure factor) and well-established parameters in the fluid dynamics of jets and fountains (Froude number). Recent visual observations of the Eyjafjallajökull eruption, on the other hand, revealed the potential for pulsating behaviour of mass flux at the source of weak sustained eruptions. A new model for measuring MER in real time based on video analysis has been developed. Outcomes from the application of this model confirm that unsteadiness significantly influences the mass eruption rate, and in particular, the evaluation of the total mass of particles injected into the atmosphere. In fact, it has been shown that measurement of the MER considering the most intense pulse as representative of the whole eruption would have resulted in an overestimate by about 50 %. [13]. This has important implications for monitoring of explosive eruptions: monitoring tools should be able to provide accurate time-dependent measurements of source condition, in order to produce reliable estimates of MER.

In the case of the Eyjafjallajökull eruption (that is, for the specific eruption magnitude and range of pulsation frequency), there is a substantial agreement between measured and computed MER values with simplified 1D plume models. However, this was verified only on the specific case here presented; further tests on eruptions with different properties (e.g. magnitude, pulsation frequency, etc.) should be carried out in the future. It is also not clear to what extent this pulsating behavior plays a role in large eruptions ( $MER > 10^7 \text{ kg s}^{-1}$ ).

Finally, results from sensitivity analysis carried out on simplified 1D numerical models further confirm the dependence of plume dynamics on source mass flux and, hence, the importance of reliable estimates of MER for accurate characterisation of plume height and trajectory, which are in turn used for initializing ash dispersion models. Numerical models are not only sensitive to uncertainties in source conditions, but also to the air entrainment parameterization. While there is a substantial agreement for the radial entrainment component, this is not the case for the tangential wind-induced one, for which a wide range of values are still used. This is reflected in the 1D plume model outputs, as wind plays a major role in affecting plume maximum height and trajectory, which in turn has an influence on MER estimates and on the initialization of ash dispersion models, for which 1D numerical models provide the initial distribution of ash in the atmosphere. We believe that scientific research on convective plumes should be specifically aimed at better constraining the parameterization of the wind entrainment coefficient, with both complex numerical simulations and new large-scale experiments (**Table 1**).

| Symbol       | Description                                     | Units               |
|--------------|---|---------------------|
| $C$          | Particle volumetric concentration               | -                   |
| $C_0$        | Particle volumetric concentration at the source | -                   |
| $d$          | Plume width                                     | m                   |
| $Fr_0'$      | Source densimetric Froude number                | -                   |
| $g_0'$       | Source reduced gravity                          | $\text{m s}^{-2}$   |
| $m$          | Particle mass load                              | kg                  |
| MER          | Mass eruption rate                              | $\text{kg s}^{-1}$  |
| $n$          | Solids mass fraction                            | -                   |
| $P_{atm}$    | Atmospheric pressure                            | Pa                  |
| $P_{dyn,0}$  | Dynamic pressure at the source                  | Pa                  |
| $P_{over,0}$ | Static overpressure at the source               | Pa                  |
| $P_{st,0}$   | Static pressure at the source                   | Pa                  |
| $Q$          | Mass flux of a pulse                            | $\text{kg s}^{-1}$  |
| $r_0$        | Vent radius                                     | m                   |
| $Re$         | Reynolds number                                 | -                   |
| $Ri$         | Richardson number                               | -                   |
| SME          | Specific mechanical energy                      | $\text{kJ kg}^{-1}$ |
| $t$          | Time  | s                   |
| $t_{pulse}$  | Average pulsation interval time                 | s                   |

| Symbol       | Description  | Units              |
|--------------|--|--------------------|
| $U$          | Axial plume velocity   | $\text{m s}^{-1}$  |
| $U_0$        | Exit velocity  | $\text{m s}^{-1}$  |
| $U_\epsilon$ | Entrainment velocity   | $\text{m s}^{-1}$  |
| $v$          | Vertical velocity of a pulse                                 | $\text{m s}^{-1}$  |
| $V$          | Wind speed   | $\text{m s}^{-1}$  |
| $W$          | Gas volume   | $\text{m}^3$       |
| $\alpha$     | Radial entrainment coefficient                               | -                  |
| $\beta$      | Tangential (wind) entrainment coefficient                    | -                  |
| $\Gamma$     | Overpressure factor  | -                  |
| $\Delta P$   | Gas overpressure   | Pa                 |
| $\theta$     | Inclination of the plume centreline to the horizon           | $^\circ$           |
| $\rho$       | Eruptive mixture density                                     | $\text{kg s}^{-1}$ |
| $\rho_g$     | Gas density  | $\text{kg s}^{-1}$ |
| $\rho_t$     | Tephra density   | $\text{kg s}^{-1}$ |
| $\tau$       | Time for which the mass flux has decreased by a factor $1/e$ | s                  |
| $\Omega$     | Vorticity factor   | $\text{s}^{-1}$    |

**Table 1.** Notation.

## Acknowledgements

Published with permission of the Executive Director of British Geological Survey (NERC). The research of Dr. Tobias Dürig presented in this chapter (Section 2) was supported by the EU FP7 supersite project Futurevolc and used photos and infrared (FLIR) images that were acquired by Björn Oddsson and Thordís Högnadóttir. The research of Dr. Fabio Dioguardi presented in this chapter (Section 3) was partially funded by DPC-INGV agreement 07–09 and MIUR PRIN 06. We like to thank Dr. Jacopo Taddeucci for his valuable suggestions that helped to improve the manuscript.

## Author details

Fabio Dioguardi<sup>1\*</sup>, Tobias Dürig<sup>2</sup>, Samantha L. Engwell<sup>1</sup>, Magnus T. Gudmundsson<sup>2</sup> and Susan C. Loughlin<sup>1</sup>

\*Address all correspondence to: [fabiod@bgs.ac.uk](mailto:fabiod@bgs.ac.uk)

<sup>1</sup> British Geological Survey, The Lyell Centre, Edinburgh, United Kingdom

<sup>2</sup> Nordvulk, Institute of Earth Sciences, University of Iceland, Reykjavik, Iceland

## References

- [1] Dacre H.F., Grant A.L.M., Hogan R.J., Belcher S.E., Thomson D.J., Devenish B.J., et al. Evaluating the structure and magnitude of the ash plume during the initial phase of the 2010 Eyjafjallajökull eruption using lidar observations and NAME simulations. *J. Geophys. Res.* 2011;116:D00U03. DOI: 10.1029/2011JD015608.
- [2] Bonadonna C., Folch A., Loughlin S., Puempel H. Future developments in modelling and monitoring of volcanic ash clouds: outcomes from the first IAVCEI-WMO workshop on Ash Dispersal Forecast and Civil Aviation. *Bull. Volcanol.* 2012;74(1):1–10. DOI: 10.1007/s00445-011-0508-6.
- [3] Mastin L.G., Guffanti M., Servranckx R., Webley P., Barsotti S., Dean K., et al. A multidisciplinary effort to assign realistic source parameters to models of volcanic ash-cloud transport and dispersion during eruptions. *J. Volcanol. Geotherm. Res.* 2009;186:10–21. DOI: 10.1016/j.jvolgeores.2009.01.008.
- [4] Degruyter W., Bonadonna C. Improving on mass flow rate estimates of volcanic eruptions. *Geophys. Res. Lett.* 2012;39:L16308. DOI: 10.1029/2012GL052566.
- [5] Sparks R.S.J., Bursik M.I., Carey S.N., Gilbert J.S., Glaze L.S., Sigurdsson H., et al. *Volcanic Plumes*. Chichester: Wiley & Sons; 1997.
- [6] Mastin L.G. A user-friendly one-dimensional model for wet volcanic plumes. *Geochem. Geophys. Geosyst.* 2007;8:Q03014. DOI: 10.1029/2006GC001455.
- [7] Tupper A., Oswald J.S., Rosenfeld D. Satellite and radar analysis of the volcanic-cumulonimbi at Mount Pinatubo, Philippines, 1991. *J. Geophys. Res.* 2005;110:D09204. DOI: 10.1029/2004JD005499.
- [8] Tupper A., Davey J., Stewart P., Stunder B., Servranckx R., Prata F. Aircraft encounters with volcanic clouds over Micronesia, Oceania, 2002–03. *Aust. Met. Mag.* 2006;55:289–299.
- [9] Marzano F.S., Lamantea M., Montopoli M., Di Fabio S., Picciotti E. The Eyjafjöll explosive volcanic eruption from a microwave weather radar perspective. *Atmos. Chem. Phys.* 2011;11:9503–9518. DOI: 10.5194/acp-11-9503-2011.
- [10] Björnsson H., Magnusson S., Arason P., Petersen G.N. Velocities in the plume of the 2010 Eyjafjallajökull eruption. *J. Geophys. Res. Atmos.* 2013;118:1–14. DOI: 10.1002/jgrd.50876.
- [11] Scharff L., Hort M., Varley N.R. Pulsed Vulcanian eruptions: a characterization of eruption dynamics using Doppler radar. *Geology*. 2015;43(11):993. DOI: 10.1130/G36705.1.
- [12] Gaudin D., Taddeucci J., Scarlato G., Moroni M., Freda C., Gaeta M., et al. Pyroclast Tracking velocimetry illuminates bomb ejection and explosion dynamics at Stromboli

- (Italy) and Yasur (Vanuatu) volcanoes. *J. Geophys. Res.* 2014;119(7):5384–5397. DOI: 10.1002/2014JB011096.
- [13] Dürig T., Gudmundsson M.T., Karmann S., Zimanowski B., Dellino P., Rietze M., et al. Mass eruption rates in pulsating eruptions estimated from video analysis of the gas thrust-buoyancy transition – a case study of the 2010 eruption of Eyjafjallajökull, Iceland. *Earth Planet Space* 2015;67:180. DOI: 10.1186/s40623-015-0351-7.
- [14] Dürig T., Gudmundsson M.T., Dellino P. Reconstruction of the geometry of volcanic vents by trajectory tracking of fast ejecta – the case of the Eyjafjallajökull 2010 eruption (Iceland). *Earth Planet Space* 2015;67:64. DOI: 10.1186/s40623-015-0243-x.
- [15] Gudmundsson M.T., Thordarson Th., Höskuldsson A., Larsen G., Björnsson H., Prata F.J., et al. Ash generation and distribution from the April-May 2010 eruption of Eyjafjallajökull, Iceland. *Sci. Rep.* 2012;2:572. DOI: 10.1038/srep00572.
- [16] Dellino P., Gudmundsson M.T., Larsen G., Mele D., Stevenson J.A., Thordarson Th., et al. Ash from the Eyjafjallajökull eruption (Iceland): fragmentation processes and aerodynamic behavior. *J. Geophys. Res.* 2012;117:B00C04. DOI: 10.1029/2011JB008726.
- [17] Ripepe M., Bonadonna C., Folch A., Delle Donne D., Lacanna G., Marchetti E., et al. Ash-plume dynamics and eruption source parameters by infrasound and thermal imagery: the 2010 Eyjafjallajökull eruption. *Earth Planet. Sci. Lett.* 2013;366:112–121. DOI: 10.1016/j.epsl.2013.02.005.
- [18] Sparks R.S.J. The dimensions and dynamics of volcanic eruption columns. *Bull. Volcanol.* 1986;48:3–15.
- [19] Patrick M.R., Harris A.J.L., Ripepe M., Dehn J., Rothery D.A., Calvari S. Strombolian eruptive styles and source conditions: insights from thermal (FLIR) video. *Earth Planet. Sci. Lett.* 2007;69:769–784. DOI: 10.1007/s00445-006-0107-0.
- [20] Marchetti E., Ripepe M., Harris A.J.L., Delle Donne D. Tracing the differences between Vulcanian and Strombolian explosions using infrasonic and thermal radiation energy. *Earth Planet. Sci. Lett.* 2009;279:273–281. DOI: 10.1016/j.epsl.2009.01.004.
- [21] Wilson L., Walker G.P.L. Explosive volcanic eruptions—VI. Ejecta dispersal in Plinian eruptions: the control of eruption conditions and atmospheric properties. *Geophys. J. R. Astron. Soc.* 1987;89:657–679.
- [22] Burgisser A., Bergantz G.W., Breidenthal R.E. Addressing complexity in laboratory experiments: the scaling of dilute multiphase flows in magmatic systems. *J. Volcanol. Geotherm. Res.* 2005;141:245–265. DOI: 10.1016/j.jvolgeores.2004.011.001.
- [23] Dellino P., Zimanowski B., Büttner R., La Volpe L., Mele D., Sulpizio R. Large-scale experiments on the mechanics of pyroclastic flows: design, engineering and first results. *J. Geophys. Res.* 2007;112:B04202. DOI: 10.1029/2006JB004313.

- [24] Dellino P., Dioguardi F., Zimanowski B., Büttner R., Mele D., La Volpe L., et al. Conduit flow experiments help constraining the regime of explosive eruptions. *J. Geophys. Res.* 2010;115:B04204. DOI: 10.1029/2009JB006781.
- [25] Dellino P., Büttner R., Dioguardi F., Doronzo D.M., La Volpe L., Mele D., et al. Experimental evidence links volcanic particle characteristics to pyroclastic flow hazard. *Earth Planet. Sci. Lett.* 2010;295:314–320. DOI: 10.1016/j.epsl.2010.04.022.
- [26] Dellino P., Dioguardi F., Mele D., D'Addabbo M., Zimanowski B., Büttner R., et al. Volcanic jets, plumes and collapsing fountains: evidence from large-scale experiments, with particular emphasis on the entrainment rate. *Bull. Volcanol.* 2014;76:834. DOI: 10.1007/s00445-014-0834-6.
- [27] Graettinger A.H., Valentine G.A., Sonder I., Ross P.S., White J.D.L. Facies distribution of ejecta in analog tephra rings from experiments with single and multiple subsurface explosions. *Bull. Volcanol.* 2015;77:66. DOI: 10.1007/s00445-015-0951-x.
- [28] Lube G., Breard E.C.P., Cronin S.J., Jones J. Synthesizing large-scale pyroclastic flows: experimental design, scaling, and first results from PELE. *J. Geophys. Res.: Solid Earth* 2015;120(3):1487–1502. DOI: 10.1002/2014JB011666.
- [29] Büttner R., Dellino P., Raue H., Sonder I., Zimanowski B. Stress-induced brittle fragmentation of magmatic melts: theory and experiments. *J. Geophys. Res.* 2006;111:B08204. DOI: 10.1029/2005JB003958.
- [30] Dürig T., Dioguardi F., Büttner R., Dellino P., Mele D., Zimanowski B. A new method for the determination of the Specific Kinetic Energy (SKE) released to pyroclastic particles at magmatic fragmentation: theory and first experimental results. *Bull. Volcanol.* 2012;74:895-902. DOI: 10.1007/s00445-011-0574-9.
- [31] Valentine G.A. Eruption column physics. In: Freundt A., Rosi M., editors. *From Magma to Tephra: modelling physical processes of explosive volcanic eruptions*. New York: Elsevier Science; 1998. p. 91-138.
- [32] Morton B.R., Taylor G., Turner J.S. Turbulent gravitational convection from maintained and instantaneous sources. *Proc. R. Soc. A.* 1956;234(1196):1-23.
- [33] Zimanowski B. Phreatomagmatic explosions. In: Freundt A., Rosi M., editors. *From Magma to Tephra: modelling physical processes of explosive volcanic eruptions*. New York: Elsevier Science; 1998. p. 25–53.
- [34] Papale P. Dynamics of magma flow in volcanic conduits with variable fragmentation efficiency and non-equilibrium pumice degassing. *J. Geophys. Res.* 2001;106(B6): 11043-11065.
- [35] Dioguardi F., Dellino P., de Lorenzo S. Integration of large-scale experiments and numerical simulations for the calibration of friction laws in volcanic conduit flows. *J. Volcanol. Geotherm. Res.* 2013;250:75-90. DOI: 10.1016/j.jvolgeores.2012.09.011.

- [36] Bloomfield L.J., Kerr R.C. A theoretical model of a turbulent fountain. *J. Fluid Mech.* 2000;424:197-216. DOI: 10.1017/S0022112000001907.
- [37] Kaye N.B., Hunt G.R. Weak fountains. *J. Fluid Mech.* 2006;558:319-328. DOI: 10.1017/S0022112006000383.
- [38] Suzuki Y.J., Koyaguchi T. 3-D numerical simulations of eruption column collapse: effect of vent size on pressure-balanced jet/plumes. *J. Volcanol. Geotherm. Res.* 2012;221-222:1-12. DOI: 10.1016/j.jvolgeores.2012.01.013.
- [39] Degruyter W., Bonadonna C. Impact of wind on the condition for column collapse of volcanic plumes. *Earth Planet. Sci. Lett.* 2013;377:218-226. DOI: 10.1016/j.epsl.2013.06.041.
- [40] Carazzo G., Kaminski E., Tait S. On the dynamics of volcanic columns: a comparison of field data with a new model of negatively buoyant jets. *J. Volcanol. Geotherm. Res.* 2008;178(1):94-103. DOI: 10.1016/j.jvolgeores.2008.01.002.
- [41] Turner J.S. Jets and plumes with negative or reversing buoyancy. *J. Fluid Mech.* 1966;26:779-792. DOI: 10.1017/S0022112066001526.
- [42] Lin W., Armfield S.W. Direct simulation of weak axisymmetric fountains in a homogeneous fluid. *J. Fluid Mech.* 2000;403:67-88. DOI: 10.1017/S0022112099006953.
- [43] Wilson L., Sparks R.S.J., Walker G.P.L. Explosive volcanic eruptions – IV. The control of magma properties and conduit geometry on eruption column behaviour. *Geophys. J. Roy. Astron. Soc.* 1980;63:117-148.
- [44] Woods A.W. The fluid dynamics and thermodynamics of eruption columns. *Bull. Volcanol.* 1988;50:169-193. DOI: 10.1007/BF01079681.
- [45] Costa A., Suzuki Y.J., Cerminara M., Devenish B.J., Esposti Ongaro T., Herzog M., et al. Results of the eruptive column model inter-comparison study. *J. Volcanol. Geotherm. Res.* In press. DOI: 10.1016/j.jvolgeores.2016.01.017.
- [46] Kaminski E., Tait S., Carazzo G. Turbulent entrainment in jets with arbitrary buoyancy. *J. Fluid Mech.* 2005;526:361-376. DOI: 10.1017/S0022112004003209.
- [47] Bursik M. Effect of wind on the rise height of volcanic plumes. *Geophys. Res. Lett.* 2001;28(18):3621-3624.
- [48] Devenish B.J. Using simple plume models to refine the source mass flux of volcanic eruptions according to atmospheric conditions. *J. Volcanol. Geotherm. Res.* 2013;256:118-127. DOI: 10.1016/j.jvolgeores.2013.02.015.
- [49] Woodhouse M.J., Hogg A.J., Phillips J.C., Sparks R.S.J. Interaction between volcanic plumes and wind during the 2010 Eyjafjallajökull eruption, Iceland. *J. Geophys. Res.: Solid Earth* 2013;118(1):92-109. DOI: 10.1029/2012JB009592.

- [50] Woodhouse M.J., Hogg A.J., Phillips J.C. A global sensitivity analysis of the PlumeRise model of volcanic plumes. *J. Volcanol. Geotherm. Res.* In press. DOI: 10.1016/j.jvolgeores.2016.02.019.
- [51] Suzuki Y.J., Koyaguchi T. Effects of wind on entrainment efficiency in volcanic plumes. *J. Geophys. Res.: Solid Earth* 2015;120(9):6122–6140. DOI: 10.1002/2015JB012208.
- [52] National Science Foundation. Vhub.org. Collaborative volcano research and risk mitigation [Internet]. Available from: <https://vhub.org>.
- [53] de' Michieli Vitturi M., Neri A., Barsotti S. PLUME-MoM 1.0: a new integral model of volcanic plumes based on the method of moments. *Geosci. Model Dev.* 2015;8(8): 2447-2463. DOI: 10.5194/gmd-8-2447-2015.
- [54] Herzog M., Graf H.F., Textor C., Oberhuber J.M. The effect of phase changes of water on the development of volcanic plumes. *J. Volcanol. Geotherm. Res.* 1998;87(1):55-74. DOI: 10.1016/S0377-0273(98)00100-0.
- [55] Cerminara M., Esposti Ongaro T., Berselli L.C. ASHEE-1.0: a compressible, equilibrium-Eulerian model for volcanic ash plumes. *Geosci. Model Dev.* 2016;9(2):697-730. DOI: 10.5194/gmd-9-697-2016.
- [56] Hewett T.A., Fay J.A., Hoult D.P. Laboratory experiments of smokestack plumes in a stable atmosphere. *Atmos. Environ.* 1971;5:767-789.
- [57] Devenish B.J., Rooney G.C., Webster H.N., Thomson D.J. The entrainment rate for buoyant plumes in a crossflow. *Boundary-layer Meteorol.* 2010;134:411-439. DOI: 10.1007/s10546-009-9464-5.
- [58] de' Michieli Vitturi M., Engwell S.L., Neri A., Barsotti S. Uncertainty quantification and sensitivity analysis of volcanic columns models: Results from integral model PLUME-MoM. *J. Volcanol. Geotherm. Res.* In press. DOI: 10.1016/j.jvolgeores.2016.03.014.

INTECH